Electronic Supplementary Material (ESI) for Nanoscale.
This journal is © The Royal Society of Chemistry 2015

Electronic Supplementary Material (ESI) for Nanoscale.

Ultrarapid and Ultrasensitive Electrical Detection of Proteins in Three-Dimensional Biosensor with High Capture Efficiency

Bo-Yeong Kim[a], *Il-yung Sohn*[b], *Doowon Lee*[b], *Gill Sang Han*[b], *Won-Il Lee*[c], *Hyun Suk Jung*[b], *Nae-Eung Lee*[a,b,c,*]

Supplementary Figure S1

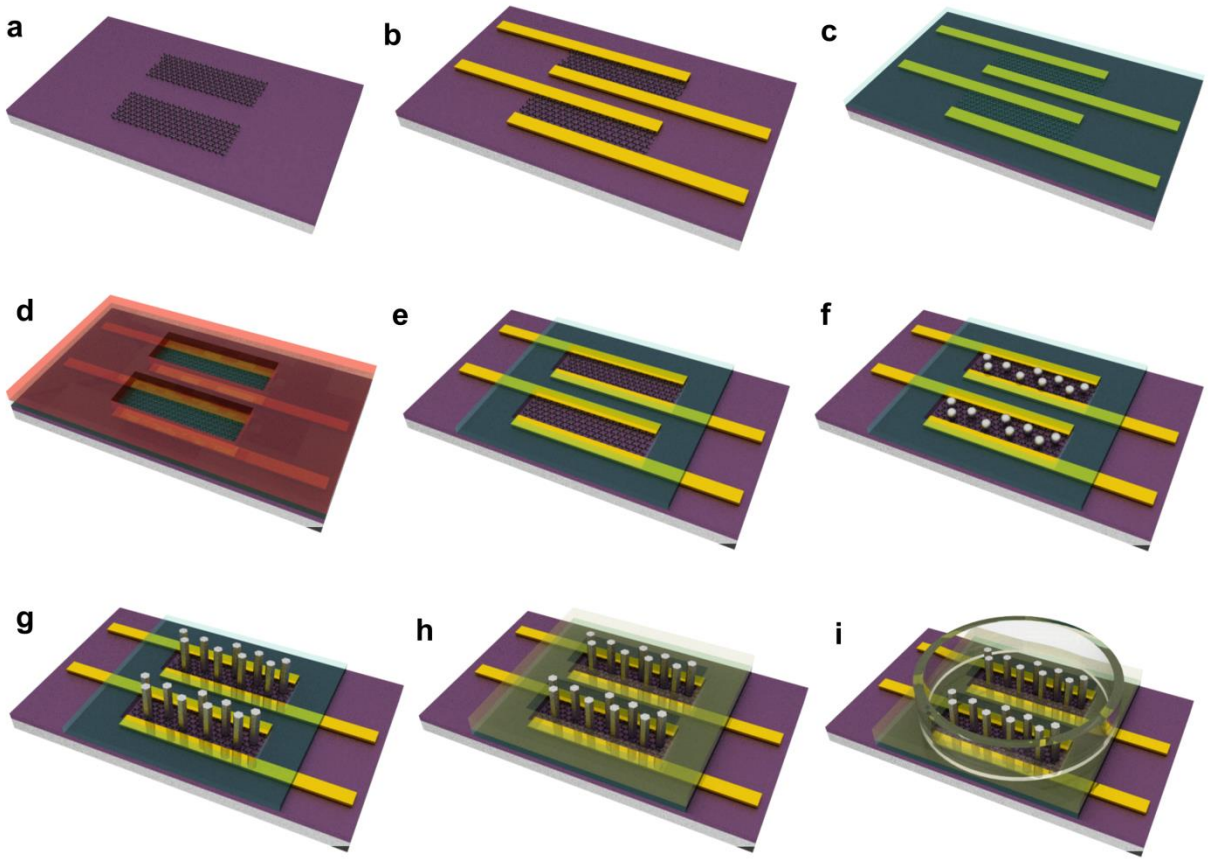

Figure S1. Device fabrication process of 3D channel bio-FET.

Supplementary Figure S2

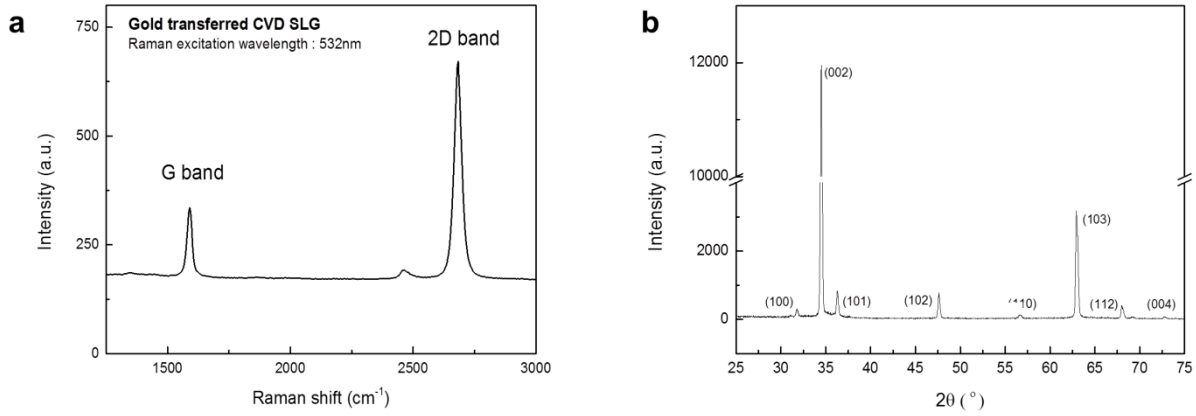

Figure S2. (a) Raman spectra of SLG transferred on SiO_2/Si wafer. (b) XRD spectra of ZnO NRs vertically grown on SLG surface.

Characterization of the Au-transferred Gr was carried out using a Raman spectrometer equipped with a 532-nm laser. **Figure S2a** shows the Raman spectra of Au-transferred Gr on the SiO_2/Si substrate, which presents the G band (~1582 cm^{-1}), the 2D band (~2700 cm^{-1}), and the D band (~1350 cm^{-1}). The notable G band originates from first-order Raman scattering, while D and 2D bands are generated from second-order Raman scattering. The intensity ratio of I_{2D}/I_G is normally 1-4 from a Gr, and the intensity of the D band is related to Gr defects.[1-3] The I_{2D}/I_G intensity ratio obtained from the Raman spectra of the Au-transferred Gr was ~2, which indicates the presence of single-layer Gr (SLG). The D band peak was very low. Therefore, the Au-transferred Gr is a high-quality SLG with a low defect density. The surface cleanness of the Au-transferred Gr could improve device properties and provide a better platform for further functionalization of the Gr surface with biomolecules or other nanostructures.

Vertical ZnO NRs were grown on the SLG surface by a solution growth method. Their diameter and height depend on growth temperature, time, and concentration of the source.[4-6] Crystallographic information from the vertically grown ZnO NRs was investigated using X-ray diffraction (XRD) (**Figure S2b**). The observed 2θ peaks located at 31.7, 34.5, 36.4, 47.5, 62.9 and 68^{o} match well with the diffraction peaks from the (100), (002), (101), (102), (110), (103) and (112) planes, respectively. The matched planes correspond to the würtzite structure of ZnO NRs, as previously reported.[7,8] The large intensity of the (002) peak is found in vertically structured ZnO NRs along the c-axis, while the (100) and (101) peaks originate from tilted ZnO NRs. The results indicate that ZnO NRs are vertically grown on the SLG by a solution growth method.

Supplementary Figure S3

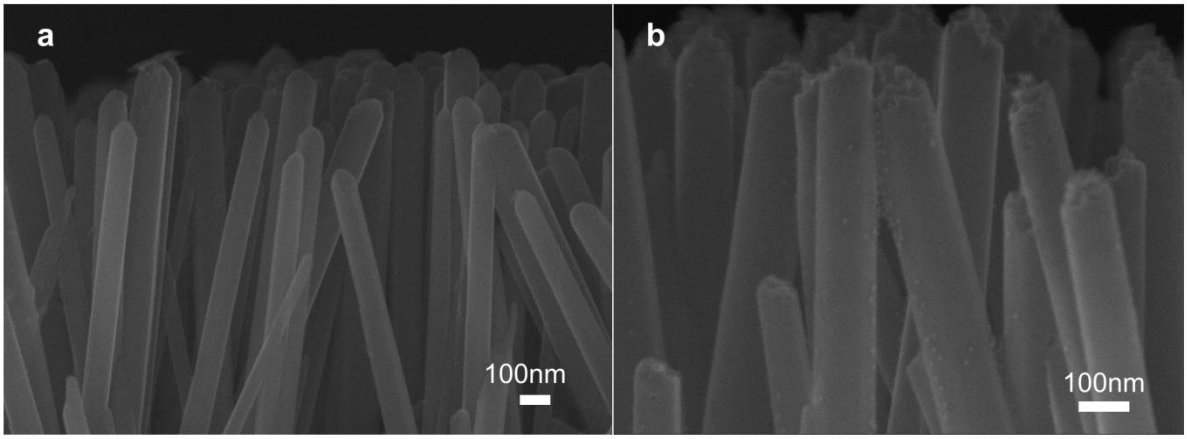

Figure S3. (a) Dissolved and etched ZnO NRs during treatment with the linker molecule solution. (b) Dissolved and etched surfaces of ZnO NRs after immobilization of probe molecules and treatment with biotin-AuNPs.

When ZnO NRs are exposed to aqueous environments they eventually dissolve, which makes probe immobilization difficult and stability of the 3D channel FET poor. The ZnO NRs were dissolved during treatment of the 3D channel with a solution of linker molecules, and the density of probe molecules was confirmed to be very low using streptavidin and biotin-grafted Au nanoparticles (biotin-AuNPs). There have been some reports on the dissolution characteristics of ZnO NRs in human sera as well as in acidic and basic solutions.[9] Therefore, capping of ZnO NRs using an ultrathin TiO_2 layer by ALD was carried out in order to passivate the surface of the ZnO NRs. A TiO_2 layer was chosen due to its stability in aqueous environments and its similar band gap of ~3.4 eV. Since the sensitivity significantly deteriorated with a thicker TiO_2 layer, the thickness of the TiO_2 layer was limited to approximately 1 nm.[10]

Supplementary Figure S4

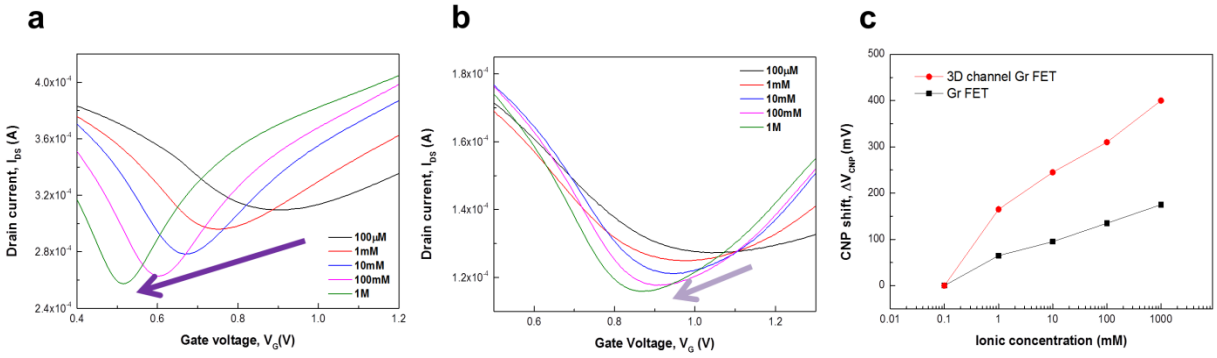

Figure S4. Transfer characteristics of (a) 3D channel FETs and (b) 2D channel FETs obtained for various ionic concentrations. Ionic concentrations varied from 100 μM to 1 M. (c) The CNP shift with increasing ionic concentrations obtained from the transfer characteristics.

The transfer characteristics were obtained at a source-drain voltage (V_{DS}) of 0.1 V by applying V_G using a platinum wire immersed in the solution as a gate electrode. Because SLG in the 3D channel FET is directly connected to the source and drain electrodes without electrical contact between the electrodes with ZnO NRs, the transfer characteristics of the 3D channel are primarily controlled by carrier transport through the SLG. This enables the detection of biomolecular interactions on the surface of ZnO NRs that induce changes in the transport properties of the SLG channel. The changes in the slope of the p- and n-branches of the transfer characteristics from the 3D channel FET was larger than that of the Gr FET, which indicates a larger coupling of ionic charge variation on the surface of TiO_2-encapped ZnO NRs in the electrolyte.

Supplementary Figure S5

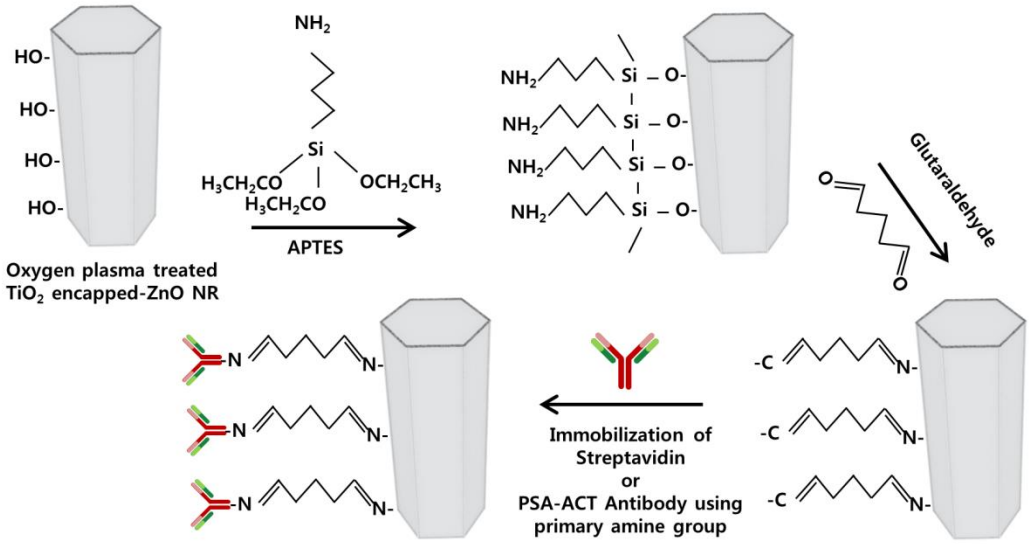

Figure S5. A schematic illustration of the immobilization steps for probe molecules (streptavidin and PSA-ACT complex antibody) on TiO_2-encapped ZnO NRs in the 3D channel FET using APTES, glutaraldehyde, and probe biomolecules.

The surface of TiO_2-encapped ZnO NRs was functionalize via treatment with (3-aminopropyl)triethoxysilane (APTES) and glutaraldehyde (GA) for attachment of probe antibodies (**Figure S5**).[11] Prior to APTES application, oxygen plasma treatment was employed to produce -OH groups on the TiO_2 surface. The amine ($-NH_2$)-terminated APTES was self-assembled on the TiO_2-encapped ZnO NRs surface with plentiful -OH groups. Terminated amine groups were activated at 150^{o}C to increase reactivity. The activated amine groups reacted with GA, which has −CHO groups on both side terminals, and thus can be linked to the primary amines of streptavidin or of the PSA-ACT antibody.

Supplementary Figure S6

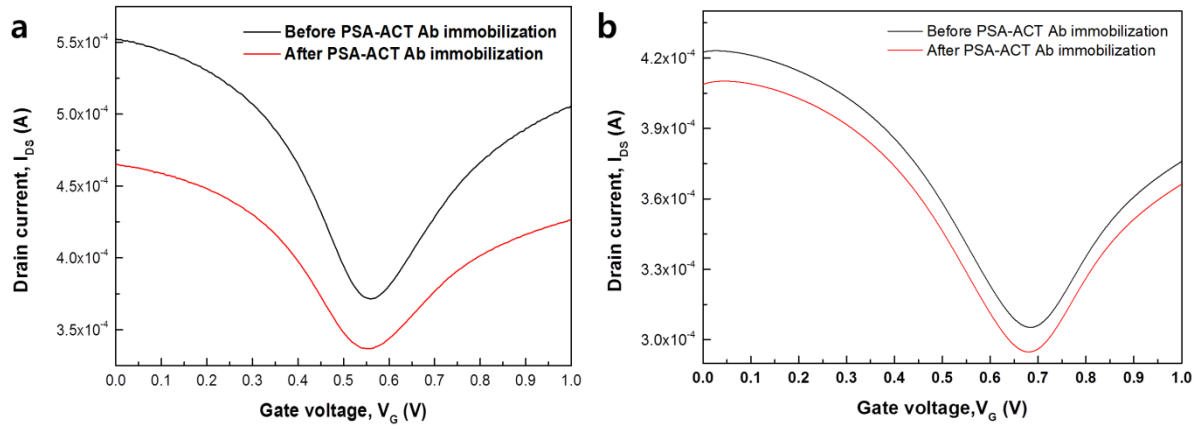

Figure S6. The transfer characteristics before and after immobilizing PSA-ACT Ab probe molecules on (a) 3D and (b) 2D channel FET, repectively.

Supplementary Figure S7

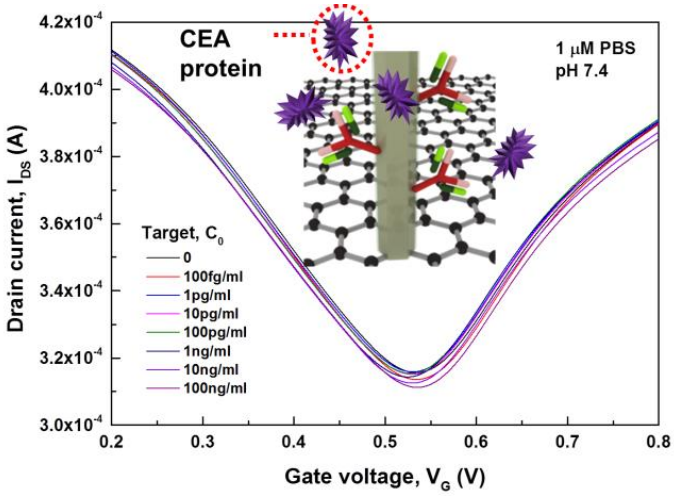

Figure S7. The transfer characteristics of 3D channel FET with immobilized PSA-ACT antibody as adding carcinoembryonic antigen (CEA) solution with the same wide range of concentration from 100 fg/ml to 100 ng/ml during the reaction time of 10 min.

Supplementary Figure S8

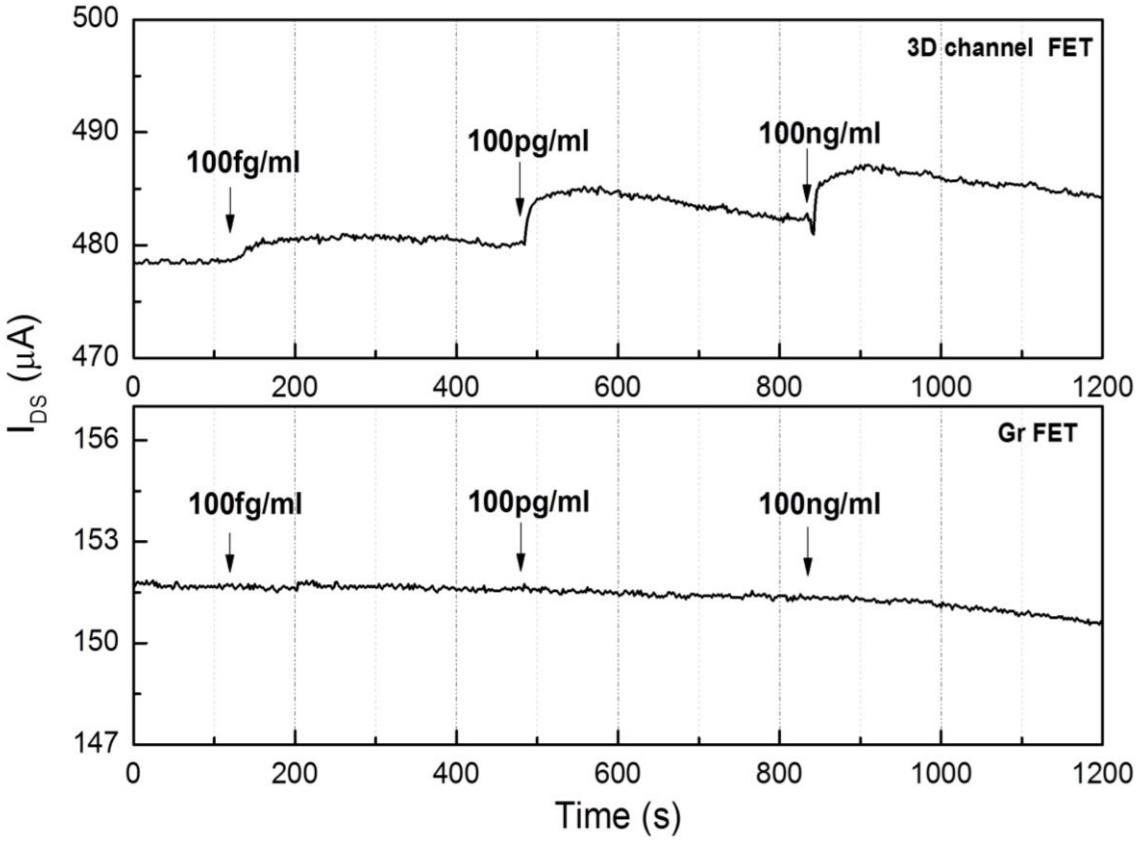

Figure S8. Time-dependent responses of 3D and 2D channel FETs adding different concentrations of analyte solution for 120, 480, and 840 s and measuring kinetics.

Supplementary Figure S9

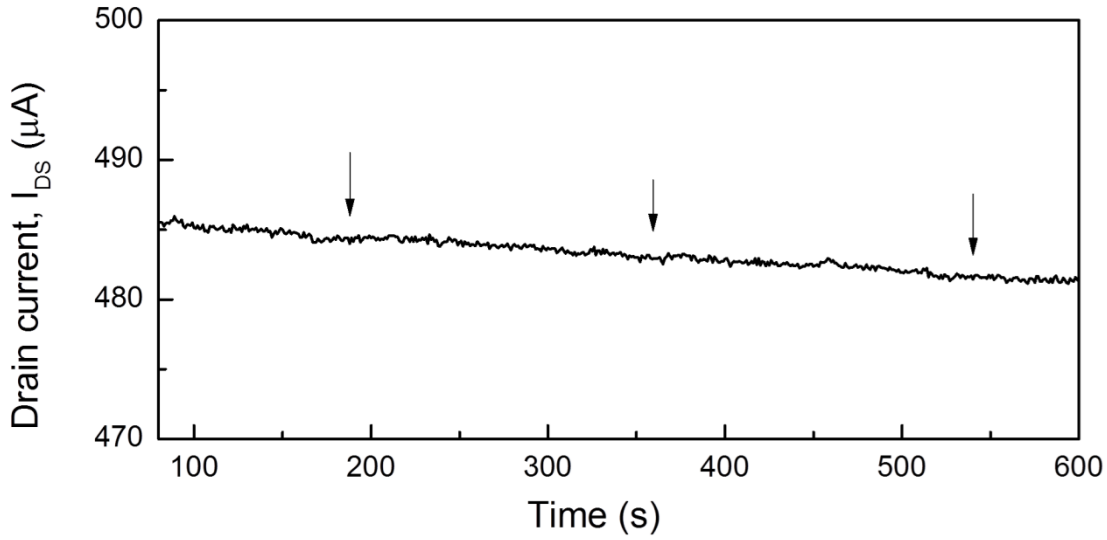

Figure S9. The drain current (I_{DS}) monitored from the 3D channel FETs during addition of a 10μl volume of PBS solution without analytes at 180, 360, and 540 s. There was no significant change in I_{DS}.

Supplementary Figure S10

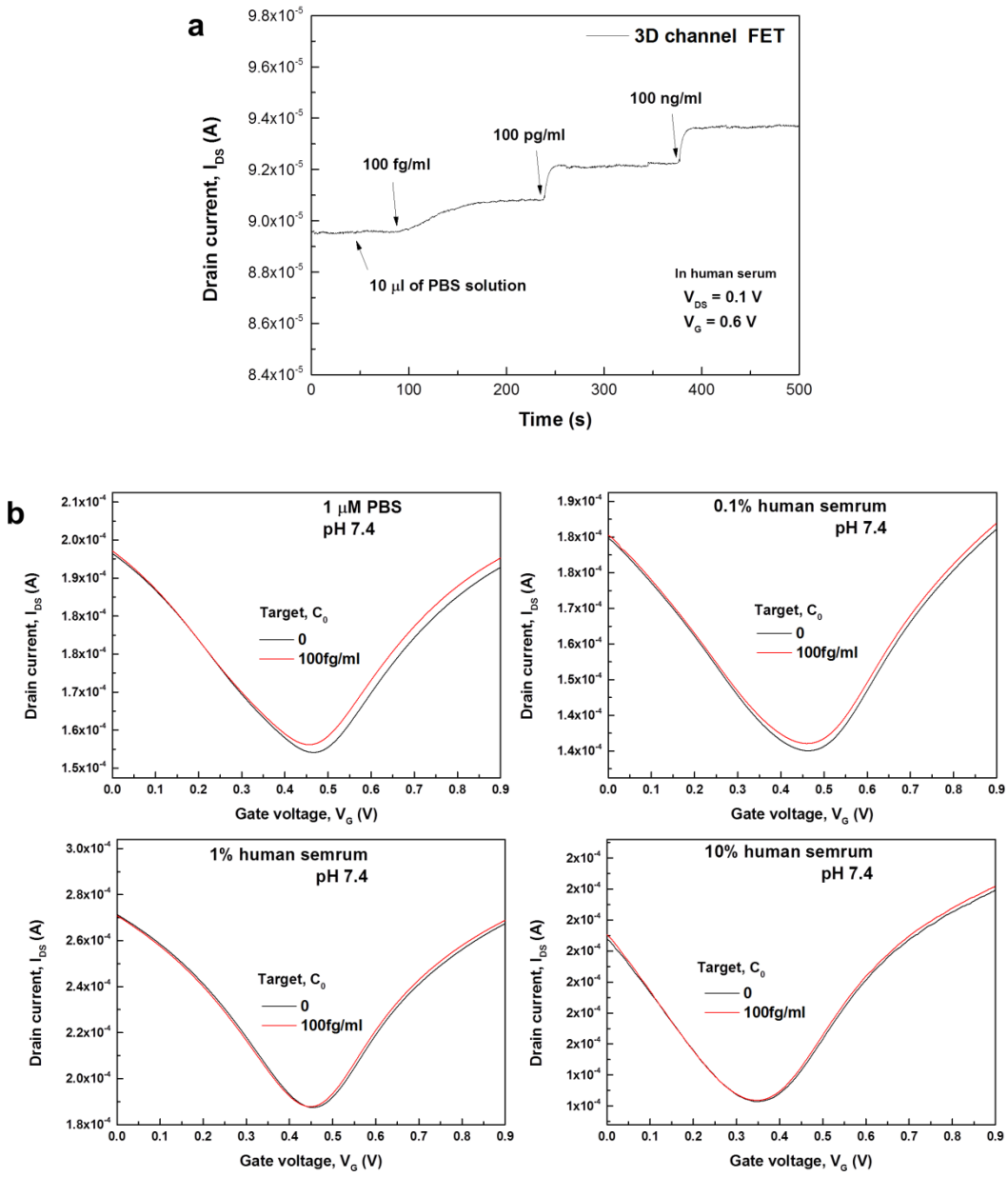

Figure S10 (a) The drain current (I_{DS}) monitored from the 3D channel FET as 100 fg/ml, 100 pg/ml and 100 ng/ml concentrations of PSA-ACT complex Ag in diluted human serum (0.1%) are added. (b) The transfer characteristics of before and after adding the 100 fg/ml concentration of PSA-ACT complex Ag in 1 μM PBS solution and in diluted human serums (0.1, 1.0 and 10%, respectively). The base sensor signals were obtained in 1 μM PBS solution and in human serums (0.1, 1.0 and 10%, respectively) at the target C_o = 0 i.e. without the PSA-ACT complex Ag molecules.

Supplementary Figure S11

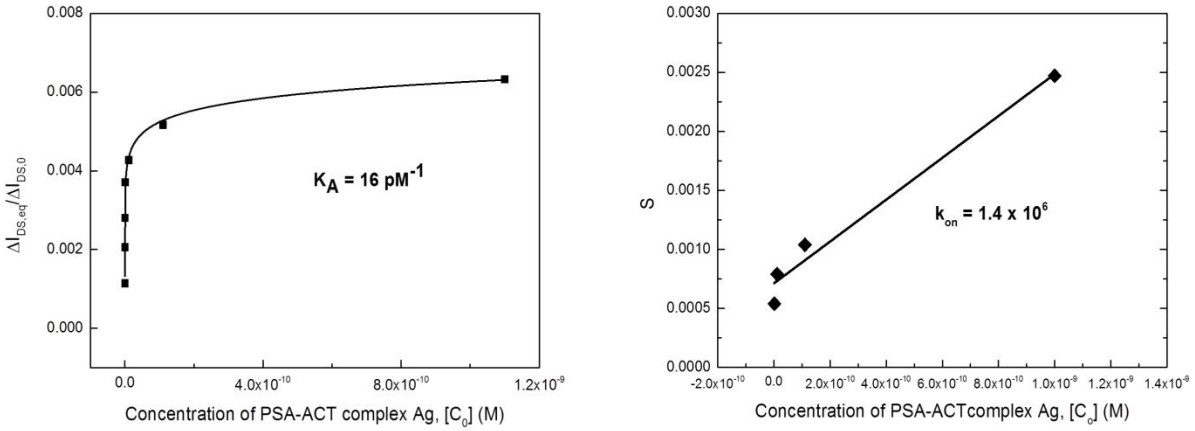

Figure S11. (a) Extraction of association constant (K_A) from the kinetic measurement data from 100 fg/ml (1.1 fM) to 100 ng/ml (1.1 nM) in Figure 4b by assuming the Langmuir isotherm. (b) Extraction of the rate of association (k_{on}) from the kinetic measurement data in **Figure 4b**. The slope of $d(\Delta I_{DS})/dt$ vs. ΔI_{DS}, S, was plotted as a function of the analyte concentration, C_o.

Based on the kinetic mêsurement data of immunoreactions (Figure 4b), the association constants, K_A, were obtained based on the Langmuir mode [12,13]. The relation is given by

$$\Delta I_{DS,eq} = \frac{\Delta I_{DS,max} K_A C_o}{1+K_A C_o}$$

where C_o is the analyte concentration in the PBS buffer, $I_{DS,eq}$ is the saturation (equilibrium) in the I_{DS} at a given C_o, and $I_{DS,max}$ is the maxium in the drain current upon immunoreaction (i.e. C_o = 0 vs. 1 nM). Fitting the data in **Figure S11a** gives a K_A value of ~16 pM^{-1}.

The slope of $d(\Delta I_{DS})/dt$ vs. ΔI_{DS}, S, obtained from the kinetic data in Figure 4b is correlated with the C_o and the rate of association (k_{on}) by the equation, $S = k_{on} C_o + k_d$

where k_d is the rate of dissociation.[13] The obtained S values were plotted as a function of C_o and the estimated slope of S vs. C_o at high C_o range gives the k_{on} value of ~10^6 M^{-1} s^{-1}.

Supplementary Figure S12

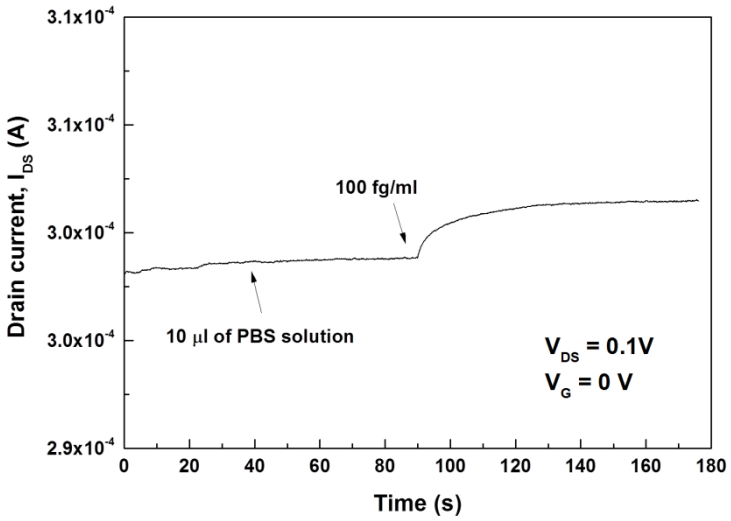

Figure S12. The drain current (I_{DS}) of 3D channel FET change as adding of 100 fg/ml of PAS-ACT complex protein along the time (s) under no gate biasing.

References

1 Ferrari A.C., *Solid State Commun.*, 2007, **143**, 47.

2 Ferrari A.C., Meyer J.C., Scardaci V., Casiraghi C., Lazzeri M., Mauri F., Piscanec S., Jiang D., Novoselov K.S., Roth S., Geim A.K., *Phys. Rev. Lett.*, 2006, **97**, 187401.

3 Cançado L.G., Pimenta M.A., Saito R., Jorio A., Ladeira L.O., Grueneis A., Souza-Filho A.G., Dresselhaus G., Dresselhaus M.S., *Phys. Rev.B: Condens. Matter Mater. Phys.*, 2002, **66**, 354151.

4 Guo M., Diao P., Cai S., *J. Solid State Chem.*, 2005, **178**, 1864.

5 Liu B., Zeng H.C., *J. Am. Chem. Soc.*, 2003, **125**, 4430.

6 Polsongkram D., Chamninok P., Pukird S., Chow L., Lupan O., Chai G., Khallaf H., Park S., Schulte A., *Phys. B(Amsterdam, Neth.)*, 2008, **403**, 3713.

7 Choi W., Shin K.-S., Lee H., Choi D., Kim K., Shin H.-J., Yoon S.-M., Choi J.-Y., Kim S.-W., *Nano Res.*, 2011, **4**, 440.

8 Guo M., Diao P., Cai S., *App. Surf. Sci.*, 2005, **249**, 71.

9 Zhou J., Xu N., Wang Z.L., *Adv. Mater.*, 2006, **18**, 2432.

10 Liu M., Nam C.-Y., Black C.T., Kamcev J., Zhang L., E., *J. Phys. Chem. C*, 2013, **117**, 13396.

11 Kim W.-J., Kim S., Lee B.S. Lee, Kim A., Ah C.S., Huh C., Sung G.Y., Yun W.S., *Langmuir*, 2009, **25**, 11692.

12 Halperin A., Buhot A., Zhulina E.B., *J. Phys.: Condens. Matter*, 2006, **18**, S463.

13 Lin A., Lee A.S.-Y., Lin C.-C., Lee C.-K, *Curr. Proteomics*, 2006, **3**, 271.